# Low-Complexity Frequency Invariant Beamformer Design Based on SRV-Constrained Array Response Control

Zihao Teng\*, Huaguo Zhang\*, Jiancheng An<sup>†</sup>, Lu Gan\*<sup>‡</sup>, Hongbin Li<sup>§</sup>, and Chau Yuen<sup>†</sup>
\*University of Electronic Science and Technology of China (UESTC), Chengdu, 611731, China

<sup>†</sup>Nanyang Technological University, 639798, Singapore

<sup>‡</sup>The Yibin Institute of UESTC, Yibin, 643000, China

<sup>§</sup>Stevens Institute of Technology, Hoboken, NJ 07030, USA

E-mail:{tzhuestc@163.com, uestczhanghuaguo@uestc.edu.cn, jiancheng.an@ntu.edu.sg,
ganlu@uestc.edu.cn, hli@stevens.edu, chau.yuen@ntu.edu.sg}

Abstract—This paper focuses on the wideband frequency invariant (FI) deterministic beamformer design problem for mitigating beam squint and presents a spatial response variation (SRV)-constrained array response control (ARC) synthesis approach. By regarding the SRV matrix as the covariance matrix of an extra virtual colored noise, we extend the ARC-based narrowband beampattern synthesis techniques to wideband FI scenarios. Furthermore, we introduce the FI maximum magnitude response (FI-MMR) based design principle, which maximizes the array magnitude response at the main-beam direction on the reference frequency. Based on this principle, we present an iterative FI beampattern synthesis algorithm under arbitrary array configurations. Simulation results show the effectiveness of the proposed algorithm in comparison with several popular FI beampattern synthesis techniques.

Index Terms—Frequency invariant (FI) beampattern, maximum magnitude response (MMR), spatial response variation (SRV), array response control (ARC)

#### I. Introduction

Wideband sensing and communication systems offer several advantages, primarily due to their high data transmission rates [1], [2]. However, directly applying narrowband arrays to wideband systems can lead to certain challenges. If the beam is focused in the normal direction, the mainlobe tends to widen at lower frequencies, impacting the system's anti-interference performance. Furthermore, if the beam is focused away from the normal direction, a phenomenon known as beam squint [3]-[5] occurs. Several techniques [6]-[8] have been presented to address this issue. Besides, frequency invariant (FI) deterministic beamformer design, also known as FI beampattern synthesis, can also be utilized for mitigating beam squint [9]. This approach is realized by employing finite impulse response (FIR) filters in the time domain. Several effective techniques for FI beampattern synthesis have been proposed in the last decades. For instance, least-squares approaches [10], [11] are able to synthesize a FI beampattern with a low sidelobe level, but cannot achieve precise sidelobe control.

The work of H. Li was supported by the National Science Foundation under grant ECCS-1923739, ECCS-2212940, and CCF-2316865.

Convex optimization based methods [12], [13] are capable of realizing precise sidelobe control, yet at the cost of high computational complexity. Additionally, fast Fourier transform (FFT) based methods [14], [15] and the generalized matrix pencil method [16] can realize FI beampattern synthesis with a low computational complexity, which, however, requires a reference narrowband beampattern. Most recently, iterative spatiotemporal Fourier transform (STFT) based methods have been proposed for FI beampattern synthesis with high implementation efficiency [17], [18]. However, they are only applicable to uniform arrays. To address this issue, the authors of [19] developed a generalized alternating projection approach (APA) for antenna arrays with arbitrary configurations. However, it comes with the trade-off of less precise control over the sidelobe level. In [20], an adaptive array theory-inspired weighted least squares (AAT-WLS) approach has been presented for wideband deterministic beamformer design with accurate beampattern control for arbitrary antenna arrays. Nevertheless, the AAT-WLS method results in high computational complexity due to the matrix inversion involved in each iteration.

Meanwhile, adaptive array theory-based array response control (ARC) techniques for beampattern synthesis have been proposed in [21], [22], offering precise control of the beampattern with low computational complexity. Nonetheless, these techniques were limited to narrowband scenarios. Motivated by the superiority of ARC, we present a new FI beampattern synthesis framework by considering a spatial response variation (SRV) constraint [23], which measures the fluctuation of the array spatial response over the desired frequency band. Specifically, we incorporate the SRV matrix as the covariance of a 'virtual colored noise' in the wideband minimum variance distortionless response (MVDR) beamformer. This 'virtual colored noise' has a correlation between different frequencyangle points that can be leveraged to realize wideband FI control. To address the phase ambiguity issue in ARC-based FI beampattern synthesis, we propose a design principle, namely the FI maximum magnitude response (FI-MMR), to determine

the optimal phase response. Armed with this principle, we present a novel FI beampattern synthesis algorithm. Simulation results show that our algorithm can realize FI beampattern synthesis under arbitrary array configurations with less CPU runtime.

#### II. ADAPTIVE ARRAY WITH SRV CONSTRAINT

Consider a wideband signal, whose frequency is bandlimited to  $f \in \mathcal{F} = [f_{\min}, f_{\max}]$ , and the temporal sampling frequency is  $f_s$ . The signal is observed by a linear wideband array with M elements, each connected to an N-tap FIR filter. Then the array response can be expressed as

$$P(f,\theta) = \mathbf{w}^H \mathbf{a}(f,\theta),\tag{1}$$

where we have

$$\mathbf{w} = [\mathbf{w}_0^{\top}, \mathbf{w}_1^{\top}, ..., \mathbf{w}_{M-1}^{\top}]^{\top} \in \mathbb{C}^{MN \times 1},$$
(2)  
$$\mathbf{h}_{f,\theta} = [g_1(f,\theta)e^{-j2\pi f \tau_1(\theta)}, ..., g_M(f,\theta)e^{-j2\pi f \tau_M(\theta)}]^{\top}$$
$$\in \mathbb{C}^{M \times 1},$$
(3)

$$\mathbf{a}(f,\theta) = \mathbf{e}_f \otimes \mathbf{h}_{f,\theta} \in \mathbb{C}^{MN \times 1},\tag{4}$$

$$\mathbf{w}_{m} = [w_{m,0}, w_{m,1}, ..., w_{m,N-1}]^{\top} \in \mathbb{C}^{N \times 1}, \tag{5}$$

$$\mathbf{w}_{m} = [w_{m,0}, w_{m,1}, ..., w_{m,N-1}]^{\top} \in \mathbb{C}^{N \times 1},$$

$$\mathbf{e}_{f} = [e^{j\pi(N-1)f/f_{s}}, ..., e^{-j\pi(N-1)f/f_{s}}]^{\top} \in \mathbb{C}^{N \times 1},$$
(6)

 $\otimes$  denotes the Kronecker product, and  $w_{m,n}$  is the nth tap coefficient of the mth FIR filter. In addition, the propagation time delay between the mth element and the reference point is  $\tau_m(\theta) = d_m \sin \theta/c$ , where  $d_m$  is the position of the mth element, c is the speed of light, and  $g_m(f,\theta)$  denotes the pattern of the mth element, which can be obtained by actual measurement or full-wave simulation. With the timedelay structure in the filters, the beam squint can be effectively mitigated by designing the weight vector w [24].

Notice that a keystone of ARC-based methods is to use a 'virtual interference-plus-noise covariance' matrix in the minimum variance distortionless response (MVDR) beamformer to suppress the noise and interference. Specifically, the SRV matrix over a given frequency set  $\mathcal{F}$  and angle set  $\Theta$ , which is defined as

$$\mathbf{Q} = \sum_{f_i \in \mathcal{F}} \sum_{\theta_j \in \Theta} \mathbf{\Delta}(f_i, \theta_j) \mathbf{\Delta}(f_i, \theta_j)^H \in \mathbb{C}^{MN \times MN}$$
 (7)

with  $\Delta(f_i, \theta_i) \in \mathbb{C}^{MN \times 1}$  defined by

$$\Delta(f_i, \theta_j) = \mathbf{a}(f_i, \theta_j) - \mathbf{a}(f_0, \theta_j). \tag{8}$$

Since the SRV matrix is a non-diagonal-Hermitian semidefinite matrix, it can be regarded as the covariance matrix of a 'virtual colored noise' to realize FI beampattern synthesis. Hence, the following modified MVDR problem is deduced:

$$\min_{\mathbf{w}} \mathbf{w}^{H} (\mathbf{R}_{\text{IPN}} + \varepsilon \sigma_{n}^{2} \mathbf{Q}) \mathbf{w}$$
 (9a)

s.t. 
$$\mathbf{w}^H \mathbf{a}(f_0, \theta_0) = 1,$$
 (9b)

where  $\mathbf{R}_{\text{IPN}} \in \mathbb{C}^{MN \times MN}$  is the interference-plus-white-noise covariance matrix,  $f_0$  is the reference frequency, and  $\theta_0$  is the look direction,  $\varepsilon > 0$  is the power trade-off factor, and  $\sigma_n^2$  is the power of white Gaussian noise. The solution of problem (9) is given as

$$\mathbf{w}_{opt} = \beta (\mathbf{R}_{IPN} + \varepsilon \sigma_n^2 \mathbf{Q})^{-1} \mathbf{a}(f_0, \theta_0), \tag{10}$$

where  $\beta$  is a constant number.

In the scenario of a single-frequency interference at  $(f_i, \theta_i)$ , we can express  $\mathbf{R}_{\text{IPN}}$  as

$$\mathbf{R}_{\text{IPN}} = \sigma_i^2 \mathbf{a}(f_i, \theta_i) \mathbf{a}(f_i, \theta_i)^H + \sigma_n^2 \mathbf{I}, \tag{11}$$

where  $\sigma_i^2$  is the power of the interference, I is the  $MN \times$ MN identity matrix. Defining  $\tilde{\mathbf{Q}} = \mathbf{I} + \varepsilon \mathbf{Q}$  and applying the Woodbury lemma, we have

$$(\mathbf{R}_{\text{IPN}} + \varepsilon \sigma_n^2 \mathbf{Q})^{-1} = \frac{1}{\sigma_n^2} (\mathbf{I} - \frac{\Gamma \tilde{\mathbf{Q}}^{-1} \mathbf{a}_i \mathbf{a}_i^H}{1 + \Gamma \mathbf{a}_i^H \tilde{\mathbf{Q}}^{-1} \mathbf{a}_i}) \tilde{\mathbf{Q}}^{-1}, \quad (12)$$

where  $\Gamma = \sigma_i^2/\sigma_n^2$  stands for the interference-to-white-noise ratio (INR), and  $\mathbf{a}(f_i, \theta_i) = \mathbf{a}_i$  for the sake of brevity.

Substituting (12) into (10), we have

$$\mathbf{w}_{opt} = \frac{\beta}{\sigma_n^2} (\mathbf{I} - \frac{\Gamma \tilde{\mathbf{Q}}^{-1} \mathbf{a}_i \mathbf{a}_i^H}{1 + \Gamma \mathbf{a}_i^H \tilde{\mathbf{Q}}^{-1} \mathbf{a}_i}) \tilde{\mathbf{Q}}^{-1} \mathbf{a}_0, \tag{13}$$

where  $\mathbf{a}_0 = \mathbf{a}(f_0, \theta_0)$ . Further omitting the common factor  $\beta/\sigma_n^2$  for brevity, the optimal weight vector is written as

$$\mathbf{w}_{opt} = \tilde{\mathbf{Q}}^{-1}(\mathbf{a}_0 + \lambda_{opt}\mathbf{a}_i), \tag{14}$$

where the optimal complex factor  $\lambda_{opt}$  is

$$\lambda_{opt} = -\frac{\Gamma \mathbf{a}_i^H \tilde{\mathbf{Q}}^{-1} \mathbf{a}_0}{1 + \Gamma \mathbf{a}_i^H \tilde{\mathbf{Q}}^{-1} \mathbf{a}_i}.$$
 (15)

#### III. PROPOSED ALGORITHM

#### A. The FI-MMR Design Principle

From (14), we can see the optimal weight vector is related to the initial vector  $\mathbf{a}_0$ , the complex factor  $\lambda_{opt}$  and the interference vector  $\mathbf{a}_i$ . The beampattern synthesis can be realized by regarding the weight vector in the (k-1)th step as the initial vector, and modifying it iteratively to ensure that all the points of beampattern satisfy the given constraints [21]. Thus we extend (14) as

$$\mathbf{w}_k = \tilde{\mathbf{Q}}^{-1}(\mathbf{w}_{k-1} + \lambda_k \mathbf{a}_k), \tag{16}$$

where  $\mathbf{w}_{k-1}$  is the weight vector obtained at the (k-1)th step, while  $\lambda_k$  and  $\mathbf{a}_k$  are the optimal complex factor and the selected array response vector at the kth step, respectively.

To determine the weight vector  $\mathbf{w}_k$ , the array response at frequency-angle point  $(f_0, \theta_0)$  is set as a reference, and the objective is to achieve accurate ARC such that

$$\frac{|\mathbf{w}_k^H \mathbf{a}_k|}{|\mathbf{w}_k^H \mathbf{a}_0|} = \rho_k, \tag{17}$$

which means

$$\frac{\mathbf{w}_k^H \mathbf{a}_k}{\mathbf{w}_k^H \mathbf{a}_0} = \rho_k e^{j\varphi_k},\tag{18}$$

where  $\rho_k$  and  $\varphi_k$  are the magnitude response and phase response at the selected frequency-angle point  $(f_k, \theta_k)$  at the kth step. Substituting (16) into (18), we can get

$$\lambda_k = \frac{(\rho_k e^{-j\varphi_k} \mathbf{a}_0^H - \mathbf{a}_k^H) \tilde{\mathbf{Q}}^{-1} \mathbf{w}_{k-1}}{(\mathbf{a}_k^H - \rho_k e^{-j\varphi_k} \mathbf{a}_0^H) \tilde{\mathbf{Q}}^{-1} \mathbf{a}_k}.$$
 (19)

From (19), we can see that for any  $\varphi_k \in (-\pi, \pi]$ , the normalize array magnitude response at  $(f_k, \theta_k)$  can be accurately controlled to a given  $\rho_k$ , which leads to a phase ambiguity issue. In wideband sensing system, an appropriate  $\varphi_k$  can be selected by maximizing the beampattern magnitude response (MMR) at  $(f_0, \theta_0)$  to improve the target detection performance [22]:

$$\max_{\lambda_k} |P(f_0, \theta_0)| \tag{20a}$$

s.t. 
$$\mathbf{w}_k = \tilde{\mathbf{Q}}^{-1}(\mathbf{w}_{k-1} + \lambda_k \mathbf{a}_k),$$
 (20b)

$$\frac{|\mathbf{w}_k^H \mathbf{a}_k|}{|\mathbf{w}_k^H \mathbf{a}_0|} = \rho_k. \tag{20c}$$

Substituting (19) and (20b) into (20a), we have

$$|P(f_0, \theta_0)| = |\mathbf{w}_k^H \mathbf{a}_0| = |(\mathbf{w}_{k-1}^H + \lambda_k^* \mathbf{a}_k^H) \tilde{\mathbf{Q}}^{-1} \mathbf{a}_0|$$

$$= \left| \frac{\mathbf{a}_k^H \tilde{\mathbf{Q}}^{-1} (\mathbf{a}_k \mathbf{w}_{k-1}^H \tilde{\mathbf{Q}}^{-1} \mathbf{a}_0 - \mathbf{a}_0 \mathbf{w}_{k-1}^H \tilde{\mathbf{Q}}^{-1} \mathbf{a}_k)}{\mathbf{a}_k^H \tilde{\mathbf{Q}}^{-1} (\mathbf{a}_k - \rho_k e^{j\varphi_k} \mathbf{a}_0)} \right|. \tag{21}$$

From (21), the phase parameter affects only the denominator of  $|P(f_0, \theta_0)|$ . Hence, problem (20) is equivalent to

$$\min_{\varphi_k} \left| \mathbf{a}_k^H \tilde{\mathbf{Q}}^{-1} \mathbf{a}_k - \rho_k e^{j\varphi_k} \mathbf{a}_k^H \tilde{\mathbf{Q}}^{-1} \mathbf{a}_0 \right|, \qquad (22a)$$

s.t. 
$$\varphi_k \in (-\pi, \pi]$$
. (22b)

Notice that  $\tilde{\mathbf{Q}}$  is a positive definite matrix, so the solution of problem (22) is given as

$$\varphi_k = \angle (\mathbf{a}_0^H \tilde{\mathbf{Q}}^{-1} \mathbf{a}_k). \tag{23}$$

The designed optimal complex factor of the FI-MMR principle in the *k*th step is

$$\lambda_k = \frac{\left(\rho_k e^{j \angle (\mathbf{a}_k^H \tilde{\mathbf{Q}}^{-1} \mathbf{a}_0)} \mathbf{a}_0^H - \mathbf{a}_k^H\right) \tilde{\mathbf{Q}}^{-1} \mathbf{w}_{k-1}}{(\mathbf{a}_k^H - \rho_k e^{j \angle (\mathbf{a}_k^H \tilde{\mathbf{Q}}^{-1} \mathbf{a}_0)} \mathbf{a}_0^H) \tilde{\mathbf{Q}}^{-1} \mathbf{a}_k}.$$
 (24)

### B. The FI Beampattern Synthesis Algorithm

The FI beampattern is designed to have a frequency invariant mainlobe shape, and the sidelobe level in  $(f_i, \theta_s)$  is lower than a given bound  $\rho(f_i, \theta_s)$ , which means for all  $f_i \in \mathcal{F}$ ,  $\theta_s \in \Theta_s$ ,

$$P(f_i, \theta_0) = 1, |P(f_i, \theta_s)| < \rho(f_i, \theta_s),$$
 (25)

where  $(\mathcal{F}, \Theta_s)$  denotes the sidelobe region.

An iterative beampattern synthesis procedure based on (16) can be carried out as follows. At the kth step, a frequency-angle point  $(f_k, \theta_k)$  in the sidelobe region, where the array response deviates most from the constraint, is selected:

$$(f_k, \theta_k) = \arg \max_{(f_i, \theta_s) \in (\mathcal{F}, \Theta_s)} D_s(f_i, \theta_s),$$
 (26)

$$D_s(f_i, \theta_s) = \frac{|\mathbf{w}_{k-1}^H \mathbf{a}(f_i, \theta_s)|}{|\mathbf{w}_{k-1}^H \mathbf{a}_0|} - \rho(f_i, \theta_s).$$
(27)

Then the array weight vector can be updated by using the selected point along with (16) and (24). The process is repeated until a convergence is reached. The proposed FI beampattern synthesis scheme is summarized in Algorithm 1. The primary computational burden of our algorithm lies in calculating  $\lambda_k$ , leading to a low complexity of  $O\left((MN)^2\right)$  per iteration.

## Algorithm 1 Focused FI Beampattern Synthesis Scheme

**Input:**  $f_{\min}$ ,  $f_{\max}$ ,  $f_0$ ,  $\theta_0$ ,  $\rho(f,\theta)$ ,  $\mathbf{a}(f,\theta)$ ,  $\varepsilon$ 

1: Initialize  $\mathbf{w}_0 = \mathbf{a}_0, k = 1$ ;

2: Initialize  $\tilde{\mathbf{Q}}$  according to (7) and  $\tilde{\mathbf{Q}} = \mathbf{I} + \varepsilon \mathbf{Q}$ ;

3: Calculate  $\tilde{\mathbf{Q}}^{-1}$ ;

4: while  $\max_{(f_i,\theta_s)\in(\mathcal{F},\Theta_s)}\left(D_s(f_i,\theta_s)\right)>0$ 

5: Select  $(f_k, \theta_k)$  by (26) and (27);

6: Update  $\mathbf{w}_k$  by (16) and (24), where  $\rho_k = \rho(f_k, \theta_k)$ ;

7: k = k + 1;

8: **end** 

Output:  $\mathbf{w}_k$ .

# IV. SIMULATION RESULTS

In all simulations, we set  $f_0 = \sqrt{f_{\min}f_{\max}}$  and  $f_s = 2f_{\max}$  to avoid aliasing. For comparison, the frequency-variation error (FVE) defined in [25] and the maximum sidelobe level (MaxSLL) are used as benchmarks.

# A. Uniform Array with Notching in Sidelobe

The first example is an FI beampattern with a notching requirement to suppress strong spatial interferes. A uniform array with 40 isotropic elements is applied to synthesize the desired pattern, where each element is connected with a 24tap FIR filter. The FI region is set to be  $[-20^{\circ}, 20^{\circ}]$ , and the desired sidelobe level is  $\rho(f_i, \theta_s) = -20$  -dB,  $f_i \in [2, 12]$ GHz,  $\theta_s \in [-90^\circ, -20^\circ) \cup (20^\circ, 45^\circ) \cup (60^\circ, 90^\circ]$ . A -42dB notch is set in [45°, 60°] over the whole frequency band,  $\rho(f_i, \theta_s) = -42 \text{ dB}, f_i \in [2, 12] \text{ GHz}, \theta_s \in [-45^\circ, 60^\circ].$  In the proposed method, we set  $\varepsilon = 10^{-4}$ ,  $\theta_0 = 0^{\circ}$ . For the purpose of comparison, the STFT-CPR [17] and the original SRV optimization [23] algorithms are included. The beampatterns are shown in Fig. 1, and Table I lists the comparison results. Table I shows that the FI beampattern synthesized by STFT-CPR cannot reach the desired notch level, especially in the low frequencies. The FI beampattern synthesized by the proposed method and the original SRV optimization have comparative FVEs, but the proposed method is more efficient with less CPU runtime.

TABLE I PERFORMANCE COMPARISON WITH NOTCHING

Method	FVE	Notch level	CPU runtime
Proposed	1.50 dB	-42.01 dB	<b>15.07 s</b> 26.71 s 68.00 s
STFT-CPR [17]	5.38 dB	-23.05 dB	
SRV [23]	<b>1.12 dB</b>	-42.22 dB	

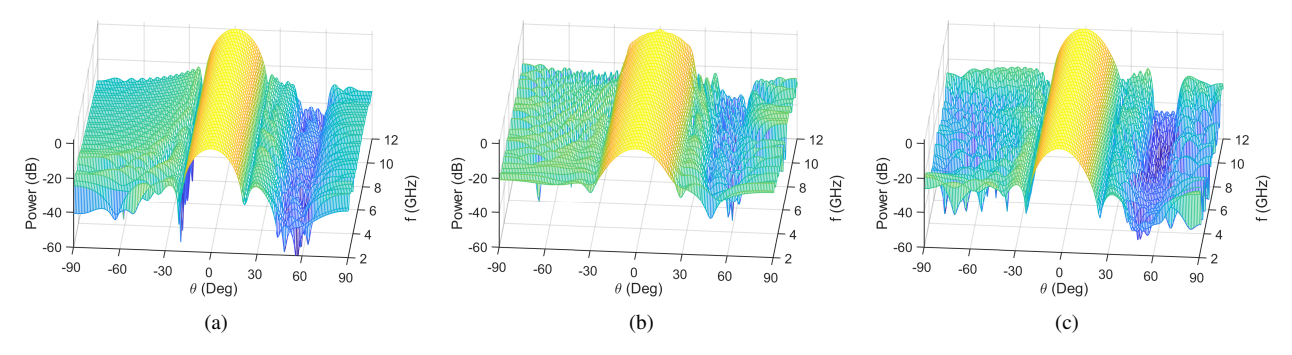


Fig. 1. Synthesized FI beampattern of a uniform array with notching. (a) The proposed method; (b) STFT-CPR; (c) The original SRV optimization.

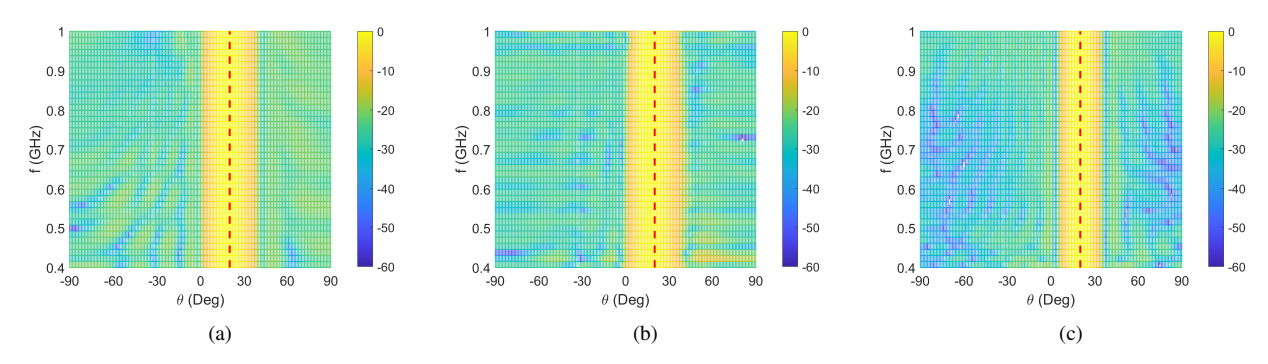


Fig. 2. Synthesized non-normal direction focused FI beampattern. (a) The proposed method; (b) STFT-CPR; (c) The original SRV optimization.

TABLE II PERFORMANCE COMPARISON IN NON-NORMAL DIRECTION FOCUSED BEAM

Method	FVE	MaxSLL	CPU runtime
Proposed	<b>0.51 dB</b>	-20.01 dB	<b>2.83 s</b> 6.18 s 14.17 s
STFT-CPR [17]	9.54 dB	-13.44 dB	
SRV [23]	0.86 dB	-20.01 dB	

# B. Non-normal Direction Focused Beam Without Squint

Next, we illustrate the performance of the non-normal direction focused FI beampattern of mitigating beam squint. Consider a 16-element uniform array, where each element is connected with a 32-tap FIR filter. The beam is focused at  $\theta_0=20^\circ$ , the FI region is set to be  $[5^\circ,35^\circ]$ , and the desired sidelobe level is  $\rho(f_i,\theta_s)=-20$  dB,  $f_i\in[0.4,1]$  GHz,  $\theta_s\in[-90^\circ,-5^\circ)\cup(35^\circ,90^\circ]$ . In the proposed method, we set  $\varepsilon=1$ . The top views of the beampatterns are presented in Fig. 2, while Table II provides a comparative analysis of the results. As observed in Fig. 2, all FI beampattern synthesis techniques effectively mitigate the beam squint phenomenon. However, the FI beampattern synthesized using the STFT-CPR method falls short of achieving the desired sidelobe level. Conversely, our proposed method not only attains the minimum FVE but also requires less CPU runtime.

# C. Nonuniform Array with Uniform Sidelobe

The last example is an FI beampattern with uniform sidelobe synthesized for a 16-isotropic-element nonuniformly spaced

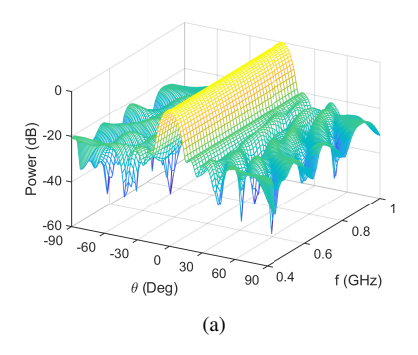
linear array, where each element is connected with a 32-tap FIR filter. Table III shows the element positions of the nonuniform array. The FI region is set to be  $[-15^\circ, 15^\circ]$ , and the desired sidelobe level is  $\rho(f_i, \theta_s) = -20$  dB,  $f_i \in [0.4, 1]$  GHz,  $\theta_s \in [-90^\circ, -15^\circ) \cup (15^\circ, 90^\circ]$ . In the proposed method, we set  $\varepsilon = 1$ ,  $\theta_0 = 0^\circ$ . Notice that [17] is only suitable in uniform arrays and [23] has a high computational complexity, the APA [19] and AAT-WLS [20] algorithms are included for comparison. The beampatterns are shown in Fig. 3, while the synthesis results are shown in Table IV. From Table IV, we can see that AAT-WLS approach fails to achieve the desired sidelobe level. The proposed method yields the lowest FVE of 0.20 dB with the shortest CPU run time of 0.84 s.

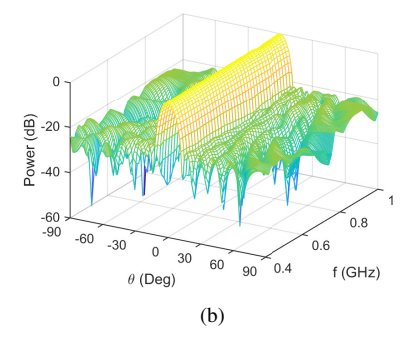
TABLE III ELEMENT POSITIONS ( $c/f_{
m max}$ ) of the Nonuniform Array

n	$d_n$	n	$d_n$	n	$d_n$	n	$d_n$
1	0.00	5	1.97	9	3.99	13	7.46
2	0.47	6	2.54	10	4.48	14	9.00
3	1.01	7	3.06	11	5.43	15	9.50
4	1.47	8	3.53	12	6.49	16	11.00

#### V. CONCLUSION

In this paper, a new SRV-constrained ARC approach was presented for FI beampattern synthesis to mitigate beam squint. Unlike the traditional narrowband ARC-based methods considering only the effect of the white noise, we introduce the SRV matrix as the covariance of a 'virtual colored noise'





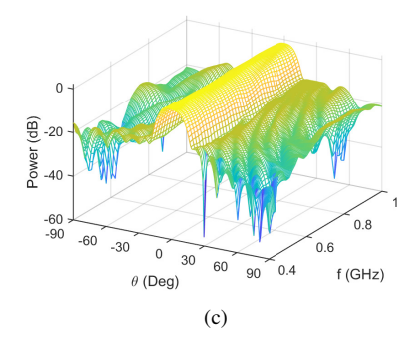


Fig. 3. Synthesized FI beampattern of a nonuniform array. (a) The proposed method; (b) APA; (c) AAT-WLS.

TABLE IV
PERFORMANCE COMPARISON IN NONUNIFORM ARRAY

Method	FVE	MaxSLL	CPU runtime
Proposed	<b>0.20 dB</b>	-20.00 dB	<b>0.84 s</b>
APA [19]	4.66 dB	-20.33 dB	6.97 s
AAT-WLS [20]	12.63 dB	-15.72 dB	21.88 s

to help realize the FI property. Moreover, we derived the FI-MMR principle to maximize the magnitude response and developed a new low-complexity algorithm for FI beampattern synthesis. Numerical results are carried out to validate the flexibility and efficiency of the proposed algorithm.

#### REFERENCES

- [1] C. Xu, J. An, T. Bai, L. Xiang, S. Sugiura, R. G. Maunder, L.-L. Yang, and L. Hanzo, "Reconfigurable intelligent surface assisted multi-carrier wireless systems for doubly selective high-mobility ricean channels," *IEEE Trans. Veh. Technol.*, vol. 71, no. 4, pp. 4023–4041, Apr. 2022.
- [2] J. An, C. Xu, D. W. K. Ng, G. C. Alexandropoulos, C. Huang, C. Yuen, and L. Hanzo, "Stacked intelligent metasurfaces for efficient holographic mimo communications in 6g," *IEEE J. Sel. Areas Commun.*, vol. 41, no. 8, pp. 2380–2396, Aug. 2023.
- [3] F. Gao, L. Xu, and S. Ma, "Integrated sensing and communications with joint beam-squint and beam-split for mmwave/thz massive mimo," *IEEE Trans. Commun.*, vol. 71, no. 5, pp. 2963–2976, May. 2023.
- [4] H. Xie, J. Palacios, and N. González-Prelcic, "Hybrid mmwave mimo systems under hardware impairments and beam squint: Channel model and dictionary learning-aided configuration," *IEEE Trans. Wirel. Commun.*, vol. 22, no. 10, pp. 6898–6913, Oct. 2023.
- [5] J. An, C. Yuen, C. Xu, H. Li, D. W. K. Ng, M. Di Renzo, M. Debbah, and L. Hanzo, "Stacked Intelligent Metasurface-Aided MIMO Transceiver Design," arXiv e-prints, p. arXiv:2311.09814, Nov. 2023.
- [6] L. Afeef and H. Arslan, "Beam squint effect in multi-beam mmwave massive mimo systems," in 2022 IEEE 96th Vehicular Technology Conference (VTC2022-Fall), 2022, pp. 1–5.
- [7] A. B. Kihero, L. Afeef, and H. Arslan, "Beam squint inspired multiple access technique in massive mimo systems," in 2022 IEEE 96th Vehicular Technology Conference (VTC2022-Fall), 2022, pp. 1–6.
- [8] J. Gou, S. Shan, and Y. Li, "Enhancement of spatial-wideband channel estimation based on beam split pattern detection," in 2023 IEEE 98th Vehicular Technology Conference (VTC2023-Fall), 2023, pp. 1–6.
- [9] W. Liu, M. Haardt, M. S. Greco, C. F. Mecklenbräuker, and P. Willett, "Twenty-five years of sensor array and multichannel signal processing: A review of progress to date and potential research directions," *IEEE Signal Process. Mag.*, vol. 40, no. 4, pp. 80–91, Jun. 2023.
- [10] G. Huang, J. Benesty, and J. Chen, "On the design of frequency-invariant beampatterns with uniform circular microphone arrays," *IEEE/ACM Trans. Audio, Speech, Language Process.*, vol. 25, no. 5, pp. 1140–1153, May. 2017.

- [11] Y. Zhao, W. Liu, and R. Langley, "Application of the least squares approach to fixed beamformer design with frequency-invariant constraints," *IET Signal Process.*, vol. 5, no. 3, pp. 281–291, Jun. 2011.
- [12] Y. Liu, J. Cheng, K. D. Xu, S. Yang, Q. H. Liu, and Y. J. Guo, "Reducing the number of elements in the synthesis of a broadband linear array with multiple simultaneous frequency-invariant beam patterns," *IEEE Trans. Antennas Propag.*, vol. 66, no. 11, pp. 5838–5848, Nov. 2018.
- [13] P. L. Son, "On the design of sparse arrays with frequency-invariant beam pattern," *IEEE/ACM Trans. Audio, Speech, Language Process.*, vol. 29, pp. 226–238, Nov. 2021.
- [14] W. Liu and S. Weiss, "Design of frequency invariant beamformers for broadband arrays," *IEEE Trans. Signal Process.*, vol. 56, no. 2, pp. 855– 860, Feb. 2008.
- [15] L. Chen, Y. Liu, S. Yang, and Y. J. Guo, "Efficient synthesis of filterand-sum array with scanned wideband frequency-invariant beam pattern and space-frequency notching," *IEEE Signal Process. Lett.*, vol. 28, pp. 384–388, Feb. 2021.
- [16] Y. Liu, L. Zhang, C. Zhu, and Q. H. Liu, "Synthesis of nonuniformly spaced linear arrays with frequency-invariant patterns by the generalized matrix pencil methods," *IEEE Trans. Antennas Propag.*, vol. 63, no. 4, pp. 1614–1625, Apr. 2015.
- [17] Y. Liu, L. Chen, C. Zhu, Y.-L. Ban, and Y. J. Guo, "Efficient and accurate frequency-invariant beam pattern synthesis utilizing iterative spatiotemporal fourier transform," *IEEE Trans. Antennas Propag.*, vol. 68, no. 8, pp. 6069–6079, Aug. 2020.
- [18] L. Chen, Y. Liu, Y. Ren, C. Zhu, S. Yang, and Y. J. Guo, "Synthesizing wideband frequency-invariant shaped patterns by linear phase response-based iterative spatiotemporal fourier transform," *IEEE Trans. Antennas Propag.*, vol. 70, no. 11, pp. 10378–10390, Nov. 2022.
- [19] L. Chen, Y. Liu, S. Yang, J. Hu, and Y. J. Guo, "Synthesis of wideband frequency-invariant beam patterns for nonuniformly spaced arrays by generalized alternating projection approach," *IEEE Trans. Antennas Propag.*, vol. 71, no. 1, pp. 1099–1104, Jan. 2023.
- [20] C. Feng and H. Chen, "Design of real-valued wideband beamformers using an adaptive-array-theory-inspired WLS: Theory and algorithm," *IEEE Trans. Signal Process.*, vol. 70, pp. 5473–5487, Mar. 2022.
- [21] X. Zhang, Z. He, B. Liao, X. Zhang, Z. Cheng, and Y. Lu, "A<sup>2</sup>RC: An accurate array response control algorithm for pattern synthesis," *IEEE Trans. Signal Process.*, vol. 65, no. 7, pp. 1810–1824, Apr. 2017.
- [22] X. Ai and L. Gan, "Single-point array response control: An efficient beampattern synthesis approach based on the maximum magnitude response principle," *IEEE Trans. Antennas Propag.*, vol. 69, no. 5, pp. 2660–2672, May. 2021.
- [23] H. Duan, B. P. Ng, M. Chong, and J. Fang, "Applications of the SRV constraint in broadband pattern synthesis," *Signal Process.*, vol. 88, no. 4, pp. 1035–1045, Apr. 2008.
- [24] W. Liu and S. Weiss, Wideband Beamforming: Concepts and Techniques. Wiley Publishing, 2010.
- [25] Z. Teng, L. Gao, L. Gan, H. Liao, K. Du, and H. Jiang, "Accurate spatial-frequency response controllable frequency invariant beampattern synthesis with minimum beamwidth," *IEEE Trans. Antennas Propag.*, vol. 71, no. 7, pp. 6266–6271, Jul. 2023.